Composite Structures 133 (2015) 1048--1057

DAMAGE EVOLUTION IN OPEN-HOLE LAMINATED COMPOSITE PLATES SUBJETED TO IN-PLANE LOADS

M. M. Moure[a], F. Otero[b], S. K. García-Castillo[a], S. Sánchez-Sáez[a], E. Barbero[a*], E. J. Barbero[a,c]

[a] Department of Continuum Mechanics and Structural Analysis, University Carlos III of Madrid, Avda de la Universidad 30, 28911 Leganés, Madrid, Spain

[b] Department of Strength of Materials and Structural Engineering, Polytechnic University of Catalonia, Spain

[c] Mechanical and Aerospace Engineering, West Virginia University, Morgantown, WV 26506, USA

*Corresponding author

Telephone number: +34 91 624 99 65

Email address: ebarbero@ing.uc3m.es

Abstract

Damage evolution of notched composite laminates is analysed in this work using a discrete damage model, which estimates matrix damage evolution and fibre failure. The fibre damage is regularized with a Weibull distribution, and a *Regula Falsi* method has been used to improve numerical convergence. The model is compared and validated with several experimental results taken from the scientific literature, which consider different materials, laminate stacking sequences and specimen geometries. A good correlation has been found for the failure strength and the stress-strain curve of notched and un-notched laminates subjected to in plane loads. The influence of the Weibull modulus on the matrix and fibre damage evolution, and the failure strength, is analysed.

Keywords: Discrete Damage Mechanics; open-hole composite laminates; ultimate strength.

1. Introduction

Failure analysis of open-hole laminates is an important subject in structural design. This problem has been extensively studied in the past, and continues to be studied nowadays due to its complexity [1-6]. The presence of a hole in a laminate is associated with stress concentration and out-of-plane stresses. These two phenomena produce a change in the failure mechanisms and a failure strength reduction of the laminate, compared to a laminate without a hole.

In the breakage of an open-hole laminate subjected to in-plane loads, several failure mechanisms can be observed: matrix cracking, fibre breakage, delamination etc. The failure mechanism which controls the breaking of the laminate depends on a large number of parameters as: material properties, laminate size and thickness, hole diameter, stacking sequence, ply thickness, width/diameter ratio, etc.

Fibre failure is a stochastic process and can be analysed using a probabilistic theory. When a single fibre breaks, a transfer of load to nearby fibres appears. Then, these fibres are subjected to a higher level of stress which increases their probability of failure. Thus, successive fibre failures may appear in the laminate until the structure fails completely [7]. Typically, fibre failure can be modelled with a Weibull distribution, both in static and fatigue problems [8-11]. The main parameter in this distribution is the Weibull modulus, which control the size of the distribution. The Weibull modulus is a material property and it is determined by experimental tests. This parameter is not easy to be determined experimentally, requiring a large number of tests, even higher than one hundred [8]. In the scientific literature, it is assumed that the most common values for the Weibull modulus of the fibres are between 3 and 9 depending on the type of fibre material [12].

Matrix cracking is an important failure mechanism, because although it does not produce the total breakage of the laminate, it degrades their mechanical properties and induces other failures modes, as delamination. Although, delamination is one of the main failure mechanisms in some open-hole laminates, as in laminates with ply level scaling [5], it is not relevant in other laminates, for example in laminates with sublaminate level scaling [13]. Matrix cracking is a complex phenomenon difficult to be modelled. Usually this is the first failure mode that appears in laminates with plies perpendicular to the load direction [10, 14-15]. The crack is initiated in defects of the interface fibre-matrix [16], these defects grow and coalesce producing an intralaminar crack transverse to ply thickness and parallel to fibre direction.

Failure strength in open-hole laminates has been estimated using analytical and numerical models [5, 6, 9, 17, 18]. Although analytical models, as the proposed by Whitney and Nuismer [17], are broadly applied in design with good results, more sophisticated models are needed to estimate the damage evolution. To model the evolution of damage in laminate composites, Fracture Mechanics or Continuous Damage Mechanics models have been used [13, 15, 19]. An alternative to these models are the Discrete Damage Models (DDM). Among these models, the proposed by

Barbero-Cortes has the advantage of modeling the matrix cracking with a single state variable [20].

In general, whatever of the previous models provides a criterion to predict the instant at which the failure of the structure takes place; for example, the point of maximum stress before a significant drop on the load-displacement curve is observed [5]. Other possibility is to define the failure at the point where a percentage of the maximum stress is achieved [21]

In this work, the behaviour of open-hole laminates subjected to in-plane loads are analysed using Barbero-Cortes DDM model. To improve the numerical convergence of this model, a *Regula Falsi* method is implemented in the matrix cracking evolution. Therefore, a new validation of the model needs to be carried out with experimental data taken from the literature, using the failure strength and laminate stiffness as variables of estimation. The failure strength of the laminates is estimated by three different criterions: Design Criterion, Local Criterion and Macro Criterion. Finally, the influence of the Weibull modulus on the failure strength and damage evolution of open-hole laminates is studied.

2. Model description

The discrete damage model (DDM) proposed by Barbero and Cortes in [20] is selected to study matrix cracking in a laminate. The method has been extended to include fibre failure [22]. The fibre failure is incorporated to the method through a simple fibre damage model that only requires one additional material property. The combined formulation is mesh independent and it has been shown to predict damage localization and laminate failure of symmetric laminates under general loads. The proposed procedure was implemented in a user general section (UGENS) in Abaqus [23].
In this section, a detailed description of the computational implementation of the method is shown. The original implementation used a modified return mapping algorithm (RMA) to estimate the growth of the crack densities in each lamina. In this work, a *Regula Falsi* method is proposed to achieve convergence for plies crack density. The original DDM described in [20] does not take into account fibre failure; therefore a short description of the fibre damage model presented in [22] is done first. The second part of this section presents the DDM formulation considering fibre damage.

2.1. Fibre failure model

The stochastic fibre strength can be represented by a Weibull distribution. If a shear lag model is used for the fibre-matrix interaction near fibre breaks, the amount of damage in the form of fibre breaks can be estimated as [12]:

$$D_1 = 1 - \exp\left[\frac{1}{m\, e}\left(\frac{\tilde{\sigma}_1}{F_{1t}}\right)^m\right] \qquad (1)$$

where m is the Weibull modulus, e is the natural log basis, F_{1t} is the longitudinal tensile strength of the unidirectional lamina, and the effective stress $\tilde{\sigma}_1$ is calculated using the longitudinal stress:

$$\tilde{\sigma}_1 = \frac{\langle \sigma_1 \rangle}{(1 - D_1)} \quad (2)$$

where $\langle x \rangle$ is the McAuley operator that returns the positive part of the argument and is used to assure that only tensile stress is used in the calculation. The fibre damage is updated only if the effective stress exceeds the tensile hardening threshold g_{1t}, which is a state variable. Then, the undamaged domain is represented by:

$$\tilde{\sigma}_1 \leq g_{1t} \quad (3)$$

Hence, when Eq. (3) is not satisfied, the damage is updated using Eq. (1) and the threshold is updated as: $g_{1t} = \tilde{\sigma}_1$. Fig. 1 shows the algorithm scheme used to implement the fibre damage model.

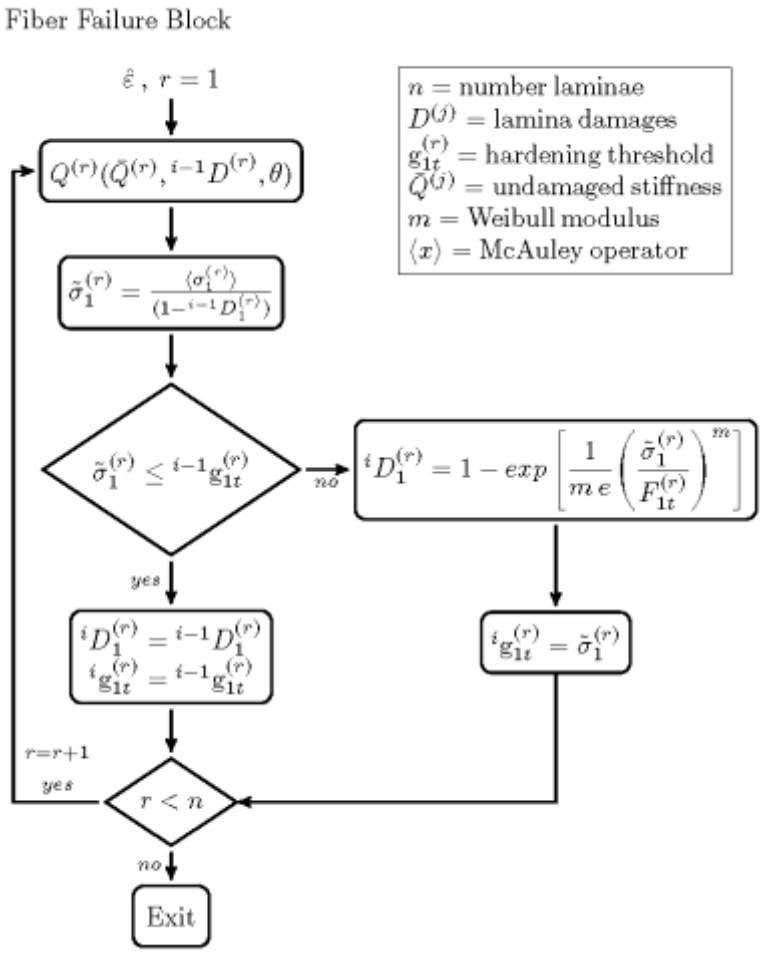

Fig.1 Fibre Failure algorithm scheme

2.2.Matrix cracking model

When the matrix is cracking, a set of parallel cracks appears. The cracking phenomenon can be represented by the crack density λ in each lamina. The crack density is the

number of cracks per unit length and it is defined as the inverse of the distance between two adjacent cracks:

$$\lambda = 1/2l \tag{4}$$

where 2l is the distance between two consecutive cracks length.
The model is formulated on a representative volume element (RVE), which is chosen as the volume enclosed by the mid-surface and top-surface of the laminate, the surfaces between two consecutive cracks 2l, and a unit length along the fibre direction parallel to the cracks [22].

The DDM works with the average thickness of the variables. A thickness average is defined as:

$$\widehat{\varphi} = \frac{1}{h}\int_h \varphi \, dx_3 \tag{5}$$

where hat denotes an average quantity and h represents the thickness over which the average is taken. Therefore, the constitutive equation and the equilibrium equations can be written in terms of the average variables.
Damage in the form of cracks is analysed as being discrete with crack density λ_k and because the discrete nature of the cracks is included, the material between cracks only is affected by fibre damage. Then, the stiffness $Q_1^{(k)}$ in the coordinates of ply k is calculated in terms of its fibre damage value $D_1^{(k)}$ and undamaged moduli as:

$$Q_1^{(k)} = \begin{bmatrix} \left(1 - D_1^{(k)}\right)\overline{Q}_{11}^{(k)} & \overline{Q}_{12}^{(k)} & 0 \\ \overline{Q}_{12}^{(k)} & \overline{Q}_{22}^{(k)} & 0 \\ 0 & 0 & \overline{Q}_{66}^{(k)} \end{bmatrix} \tag{6}$$

where overline denotes undamaged quantities and the variable $D_1^{(k)}$ represent the longitudinal stiffness reduction of the ply k. The remaining plies have damaged stiffness in the coordinated system of lamina k that can be calculated in terms of their previously calculated damage values $D_{2,6}^{(m)}$ and the fibre damage $D_1^{(m)}$ as follows:

$$Q^{(m)} = [T(\theta)]^{-1}\begin{bmatrix} \left(1 - D_1^{(m)}\right)\overline{Q}_{11}^{(m)} & \left(1 - D_2^{(m)}\right)\overline{Q}_{12}^{(m)} & 0 \\ \left(1 - D_2^{(m)}\right)\overline{Q}_{12}^{(m)} & \left(1 - D_2^{(m)}\right)\overline{Q}_{22}^{(m)} & 0 \\ 0 & 0 & \left(1 - D_6^{(m)}\right)\overline{Q}_{66}^{(m)} \end{bmatrix}[T(\theta)]^{-1} \tag{7}$$

where k and m are labels for the cracked ply and the remaining plies, respectively; $[T(\theta)]^{-1}$ is the stress transformation matrix, with the angle θ measured from k to m, and $D_1^{(m)}$ and $D_2^{(m)}$ and $D_6^{(m)}$ represent the longitudinal, transverse and shear stiffness reduction of the plies $m \neq k$.

The equilibrium equations are written and solved in terms of the average variables. Therefore, the overall reduced stiffness properties can be estimated applying unit normal and shear loads and calculating the induced deformations. In other words, the components of the laminate compliance S in the material coordinate system of the cracked lamina k are:

$$Q^{-1}(\lambda) = S(\lambda) = \left[\begin{Bmatrix} \hat{\varepsilon}_1 \\ \hat{\varepsilon}_2 \\ \hat{\gamma}_{12} \end{Bmatrix}^{(a)} \quad \begin{Bmatrix} \hat{\varepsilon}_1 \\ \hat{\varepsilon}_2 \\ \hat{\gamma}_{12} \end{Bmatrix}^{(b)} \quad \begin{Bmatrix} \hat{\varepsilon}_1 \\ \hat{\varepsilon}_2 \\ \hat{\gamma}_{12} \end{Bmatrix}^{(c)} \right] \tag{8}$$

which have been obtained considering the three unit-load cases:

$$\begin{Bmatrix} \hat{\sigma}_1 \\ \hat{\sigma}_2 \\ \hat{\tau}_{12} \end{Bmatrix}^{(a)} = \begin{bmatrix} 1 \\ 0 \\ 0 \end{bmatrix}, \quad \begin{Bmatrix} \hat{\sigma}_1 \\ \hat{\sigma}_2 \\ \hat{\tau}_{12} \end{Bmatrix}^{(b)} = \begin{bmatrix} 0 \\ 1 \\ 0 \end{bmatrix}, \quad \begin{Bmatrix} \hat{\sigma}_1 \\ \hat{\sigma}_2 \\ \hat{\tau}_{12} \end{Bmatrix}^{(c)} = \begin{bmatrix} 0 \\ 0 \\ 1 \end{bmatrix} \tag{9}$$

On the other hand, the damaged laminate stiffness can be written as:

$$Q = Q^{(k)} \frac{h^{(k)}}{H} + \sum_{m}^{n-1} Q^{(m)} \frac{h^{(m)}}{H} \tag{10}$$

where H is the laminate thickness.

The coefficients of $Q^{(k)}$ can be computed From Eq. (10) since the damaged laminate stiffness ($Q = S^{-1}$) is computed from Eq.(8) and damaged plies stiffness $Q^{(m)}$ are known by Eq.(7). Therefore, the damage variables of the cracked ply $D_{2,6}^{(m)}$ are calculated as follows:

$$\begin{aligned} D_2^{(k)}(\lambda_k) &= 1 - Q_{22}^{(k)} / \overline{Q}_{22}^{(k)} \\ D_6^{(k)}(\lambda_k) &= 1 - Q_{66}^{(k)} / \overline{Q}_{66}^{(k)} \end{aligned} \tag{11}$$

The matrix cracking damage activation function is writing in terms of the energy release rate (ERR) associated with crack opening displacements in mode I and mode II, G_I and G_{II} respectively.

$$g(\lambda_k) = (1 - r) \sqrt{\frac{G_I(\lambda_k)}{G_{IC}}} + r \frac{G_I(\lambda_k)}{G_{IC}} + \frac{G_{II}(\lambda_k)}{G_{IIC}} - 1 \leq 0 \tag{12}$$

where $r = G_{IC}/G_{IIC}$ and G_{IC} and G_{IIC} are the critical values for mode I and mode II of the ERR. This activation function works as damage initiation and also as damage-evolution criteria.

The Fig.2 shows the algorithm used to implement DDM.

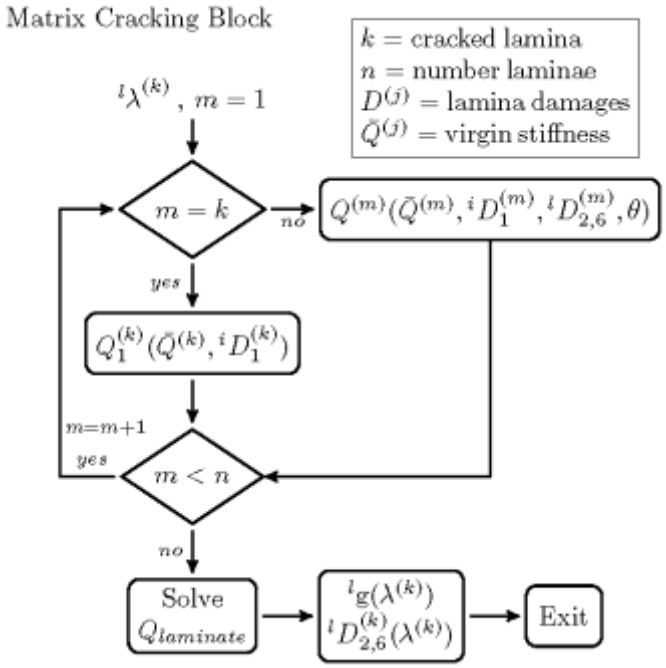

Fig.2. Matrix cracking implementation

2.3.Matrix cracking evolution

In ply k, the activation function and matrix cracking damage variables $D_{2,6}^{(k)}$ are both univocal functions of its crack density λ_k.Then, the evolution of matrix cracking damage, when matrix cracking is detected, is a function of the increment of crack density, that is $\dot{D}_{2,6}^{(k)}(\dot{\lambda}_k)$. Here, an increment of one variable is defined as, $\dot{\lambda} \equiv \Delta\lambda = \lambda - \lambda_{old}$. According to the Kuhn-Tucker conditions,

$$\dot{\lambda}_k \geq 0 \quad ; \quad g(\lambda_k) \leq 0 \quad ; \quad \dot{\lambda}_k g(\lambda_k) = 0 \qquad (13)$$

the values of $\dot{\lambda}_k$ and $g(\lambda_k)$ allow to distinguish between two possible states, loading or unloading without matrix damage growth, and loading with matrix damage growth. The two possible situations can be differentiated by:

1. Unloading or loading without damage, in the elastic domain. The activation function is $g(\lambda_k) \leq 0$, therefore the crack density increment must be $\dot{\lambda}_k = 0$ to satisfy Eq. (13).
2. Damage loading. In this state $\dot{\lambda}_k > 0$ and it implies that $g(\lambda_k) = 0$ by condition (13).

Matrix cracking is detected in ply k for case 2. At the beginning, the activation function takes a value of $g(\lambda_k) > 0$. Then, it is necessary to find the value of the new crack density ($\dot{\lambda}_k > 0$) that returns the activation function to $g(\lambda_k) = 0$. A Regula Falsi method is implemented to impose the Kuhn-Tucker conditions. Fig.3 shows the algorithm used to implement the Regula Falsi method.

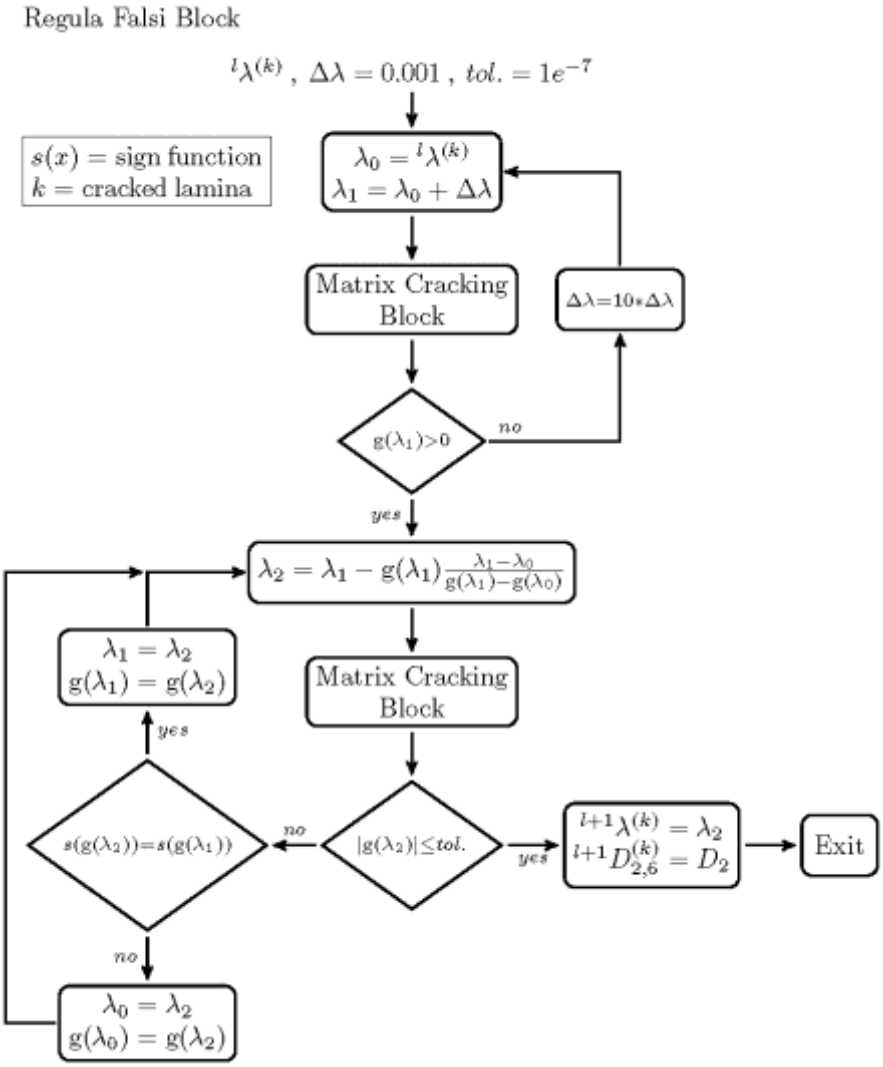

Fig.3 Regula Falsi algorithm implemented

2.4.Combined damage algorithm

Fig. 4 shows the implementation of the combined formulation on a laminate. At the beginning, fibre damage is updated in the plies using the fibre failure method described. The box with the name Fibre Failure Block uses the algorithm shown in Fig.1. After that, the updating process of transversal and shear damage is started. For each ply, the activation function is calculated and if $g(\lambda_k) > 0$ the Regula Falsi method is used to return $g(\lambda_k)$ to zero. Matrix damages are updated with the new crack density calculated. The loop over the plies continues until all plies satisfy $g(\lambda_k) \leq 0$ condition in one cycle. In other words, the plies loop stops when $nl \neq 1$ (see Fig. 4).

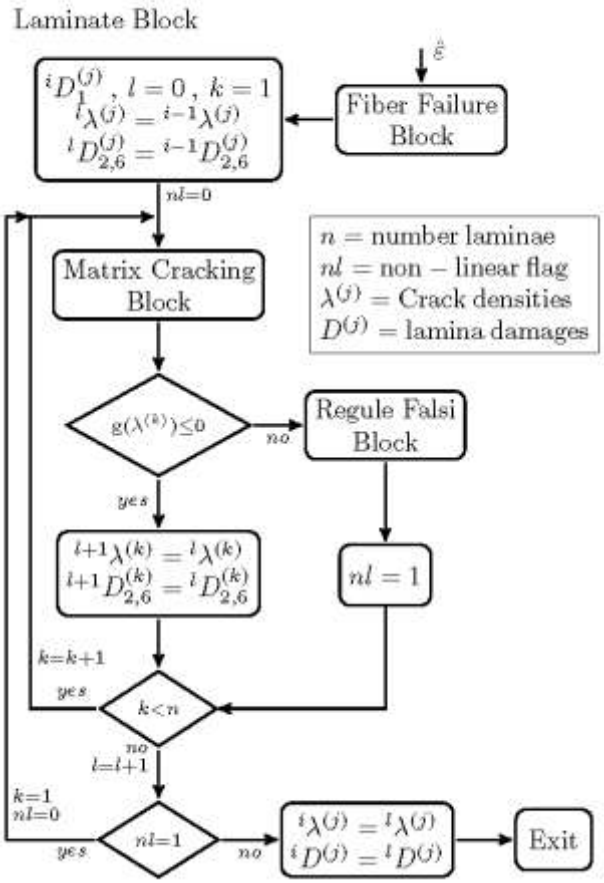

Fig. 4. Laminate implementation scheme of the combined formulation.

3. Model Validation

To improve the numerical convergence of the DDM model, a Regula Falsi method is implemented to estimate the matrix cracking evolution. Therefore, a new validation of the model is needed.

3.1.Problem Description

Notched and un-notched composite plates subjected to uniaxial tensile load are analysed. The plates have been discretized with S4 type elements as shown in Fig. 5. For notched laminates, the discretization is done so that the element size is approximately the same in all geometries studied. For un-notched laminates the plate is discretized with 900 elements.

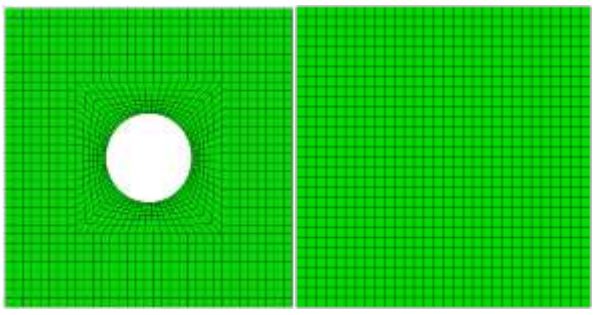

Fig. 5. Discretization of notched and un-notched laminates.

To estimate the failure strength of the laminates, three different criterions are used: Design Criterion, Local Criterion and Macro Criterion. The first criterion is often used for design when the analysis software available does not provide the other two criteria. To define each of these three criteria the longitudinal stress curve on 0º plies for the element just above the hole is needed (Fig. 6).

The Design Criterion assumes that the specimen fails when the longitudinal stress in the most loaded Gauss point reaches the fibre tensile strength (F_{1t}). The Local Criterion considers that the laminate fails when longitudinal stress in the most loaded Gauss point decreases to zero, so that the region around the Gauss point is completely damaged. Finally, the Macro Criterion assumes that the specimen fails when the maximum load and displacement that the numerical algorithm is able to apply are reached, considering longitudinal cross softening, cutting, and damage caused by the fibre and matrix, respectively. Eventually, the algorithm detects when the stiffness matrix becomes singular, which corresponds to Macro Criterion failure.

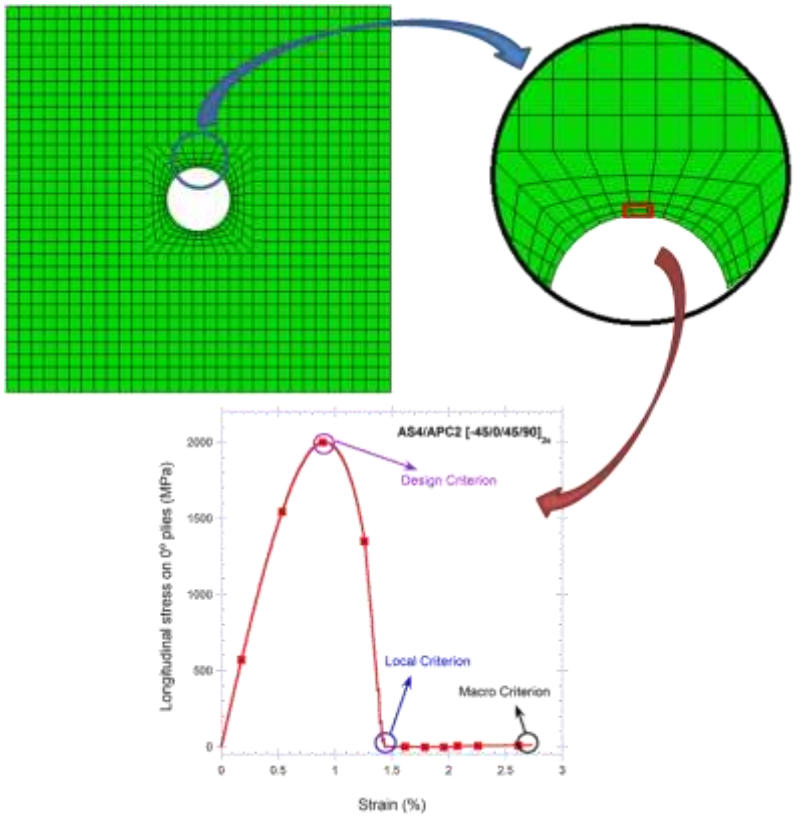

Fig. 6. Definition of the three criteria used to estimate the failure strength of the notched laminates.

In this work, the new formulation of the DDM model is extensively validated with several materials and configurations from the literature [12, 13, 24-27, 30-32]. Ten

laminates, with six different fibres (T300, T700, AS4, IM7, CCF300, and HTA) and nine matrices (1034C, 3502, 3501-6, APC2, 8552, 8911, 5228, 5428, and 6376-C), are analysed. The properties of these materials are taken from the literature and are shown in Tables 1 and 2. As the actual implementation of the DDM model does not include delamination, only laminate lay-ups with experimental evidence in the literature of no delamination or ply splitting are selected.

Table 1. Material properties of the composite materials analysed I

Property	T300/1034-C [27]	AS4/3502 [24]	AS4/3501-6 [25] (fv=0.6)	AS4/APC2 [25] (fv=0.6)	IM7/8552 [26] (fv=0.6)	IM7/8552 [13] (fv=0.6)
$E1\ (GPa)$	146.8	143.9	123	112	161	171.42
$E2\ (GPa)$	11.4	11.9	9.6	11	11.4	9.08
$G12\ (GPa)$	6.1	6.7	4.8	6.2	5.17	5.29
ν_{12}	0.3	0.326	0.31	0.32	0.32	0.32
ν_{23}	0.427	0.44	0.43	0.44	0.44	0.44[6]
$\alpha_1\ (^{o}C^{-1})$	$-1\cdot10^{-6}$	$-0.89\cdot10^{-6}$	$-1\cdot10^{-6}$	$40.2\cdot10^{-6}$ [11]	0	$-5.5\cdot10^{-6}$
$\alpha_2\ (^{o}C^{-1})$	$26\cdot10^{-6}$	$23\cdot10^{-6}$	$21.6\cdot10^{-6}$	$40.2\cdot10^{-6}$ [11]	$1\cdot10^{-5}$	$25.8\cdot10^{-6}$
$G_{IC}\ (N/mm)$	0.228	0.358[a]	0.59 [a]	0.54 [a]	0.2	0.2774
$G_{IIC}\ (N/mm)$	0.455	0.396[a]	0.89 [a]	3.65 [a]	1	0.7879
$F_{1t}\ (MPa)$	1730	1862	1600	2000	2806[13]	2326.2
$F_{1c}\ (MPa)$	1379	1482	1480[11]	1080	1200	1200.1
$F_{2t}\ (MPa)$	66.5	52	60	73.1	60[13]	62.3
$F_{2c}\ (MPa)$	268.2	207	200[11]	196	185[13]	199.8
$F_6\ (MPa)$	58.7	65	80.7	190	90[13]	92.3
$t_t\ (mm)$	0.8 [b]	0.8 [b]	0.8 [b]	0.8 [b]	0.8 [b]	0.8 [b]
$t_k\ (mm)$	0.1308	0.1308[9]	0.134[12]	0.125[12]	0.125[13]	0.131
m	3[c]	4 [c]	4 [c]	5 [c]	6 [c]	5 [c]

[a] Estimated [12, (7.39)]
[b] [12, § 7.2.1]
[c] [12, Table 2.3]

Table 2. Material properties of the composite materials analysed II

Property	CCF300/5228 [30] (fv=0.63)	CCF300/5428 [30] (fv=0.63)	T700/5428 [30] (fv=0.63)	HTA /6376-C [31]	T700/8911 [32] (fv=0.62)
$E1\ (GPa)$	137	145	125	139	135
$E2\ (GPa)$	8.8	9.75	7.8	10	11.41
$G12\ (GPa)$	4.4	5.69	5.6	5.2	7.92
ν_{12}	0.32	0.312	0.32	0.32	0.33
ν_{23}	0.46	0.44	0.46	0.51	0.33
$\alpha_1\ (^{o}C^{-1})$	$1.5\cdot10^{-7}$	$4\cdot10^{-7}$	$9.7\cdot10^{-7}$	$-1\cdot10^{-6}$	$-1\cdot10^{-6}$
$\alpha_2\ (^{o}C^{-1})$	$3.54\cdot10^{-5}$	$2.5\cdot10^{-5}$	$2.09\cdot10^{-5}$	$24\cdot10^{-6}$	$24\cdot10^{-6}$
$G_{IC}\ (N/mm)$	1.17 [a]	0.77[a]	0.85 [a]	0.26 [17]	0.50 [a]
$G_{IIC}\ (N/mm)$	2.05 [a]	1.15[a]	1.36 [a]	1.002 [17]	0.70 [a]
$F_{1t}\ (MPa)$	1744	1858	2450	2170	2600
$F_{1c}\ (MPa)$	1230	1318	1210	1600	1422
$F_{2t}\ (MPa)$	81	69	65	73	60.3

F_{2c} (MPa)	245	229	220	290	241
F_6 (MPa)	120	102	111	83	94
t_t (mm)	0.8 [b]	0.8 [b]	0.8 [b]	0.8 [b]	0.8 [b]
t_k (mm)	0.125	0.125	0.125	0.13	0.1125
m	4[c]	3 [c]	3 [c]	6 [c]	5 [c]

[a] Estimated [12, (7.39)]

[b] [12, § 7.2.1]

[c] [12, Table 2.3]

3.2.Results

The experimental failure strength of notched and un-notched laminates [13, 24-27, 30-32] is compared with numerical results obtained from DDM using the 3 criteria mentioned before (Tables 3 and 4).

Table 3. Failure strength for notched laminates.

					Num. Design Criterion		Num. Local Criterion		Num. Macro Criterion	
Material	**Stacking sequence**	***R*** **(mm)**	***W*** **(mm)**	**Exp.** σ (MPa)	σ **(MPa)**	**Error (%)**	σ **(MPa)**	**Error (%)**	σ **(MPa)**	**Error (%)**
T300/1034-C [4]	$[0/\pm45/90_7]_s$	3.175	25.4	160	132.59	**17.13**	162.12	**1.33**	190.38	**18.99**
AS4/3502 [4]	$[0/90/\pm45]_s$	3.81	25.4	326	283.09	**13.16**	313.31	**3.89**	313.31	**3.89**
AS4/3501-6 [5]	$[45/90/-45/0]_{2s}$	3.175	38.1	341 (5.28%)	255.27	**25.14**	342.76	**0.52**	364.60	**6.92**
AS4/APC2 [5]	$[-45/0/45/90]_{2s}$	3.175	38.1	357 (8.96%)	318.84	**10.69**	361.84	**1.36**	522.56	**46.38**
IM7/8552 [6]	$[45/90/-45/0]_{2s}$	3.175	32	438 (2.44%)	395.03	**9.81**	439.19	**0.27**	439.19	**0.27**
	$[45/90/-45/0]_{4s}$	3.175	32	433 (2.3%)	395.04	**8.77**	436.38	**0.78**	506.78	**17.04**
IM7/8552 [7]	$[90/0/\pm45]_{3s}$	5	60	373.7 (3.8%)	337.59	**9.66**	378.36	**0.12**	430.29	**15.14**
CCF300/5228 [8]	$[45/0/-45/90]_{3s}$	3	36	325	260.43	**19.87**	303.59	**6.59**	324.99	**0.003**
CCF300/5428 [8]	$[45/0/-45/90]_{3s}$	3	36	375	302.37	**19.37**	375.76	**0.20**	392.79	**4.74**
T700/5428 [8]	$[45/0/-45/90]_{3s}$	3	36	517	406.42	**21.39**	497.26	**3.82**	515.92	**0.21**
T700/8911 [16]	$[0/45/90/-45]_{2s}$	5	25	401	364.87	**9.01**	399.98	**0.25**	399.98	**0.25**

In all cases, the Design Criterion provides conservative results but its accuracy is not very good, being the best a 6.52%, and in most cases exceeds 10%. Although the Macro criterion shows an excellent approximation in some cases (for example for CCF300/5228 for which the error is practically nil) in other cases the approach is not good (as for AS4/APC2 for which the error is 46.38 %). The Local criterion shows very small differences with the experimental data in all cases, so it could be considered the most appropriate for use in combination with the DDM model to estimate the failure strength of materials with different types of fibres and matrices, both thermoset (epoxy) and thermoplastic (PEEK). The largest difference observed with the Local criterion is 6.59%. Although for some of the laminates the Local criterion provides unconservative results; the differences with the experimental values are lower than the experimental scatter, therefore providing an accurate estimation.

Since only three of the laminates shown in Table 3 provide experimental results of un-notched failure strength, three stacking sequences of HTA/6376-C, not included in Table 3, are analysed to extend the DDM model validation. In un-notched laminates, no stress concentration appears, so the failure estimated by the three criteria coincide, and thus a single predicted failure strength value is shown in Table 4, compared to the corresponding experimental value from the literature. For un-notched laminates, the differences are smaller than for notched laminates, being the largest 4.49%.

Table 4. Failure strength for un-notched laminates.

Material	Stacking sequence	W (mm)	Experimental σ (MPa)	Numerical σ (MPa)	Error (%)
AS4/3501-6 [5]	$[45/90/-45/0]_{2s}$	38.1	660 (6.80%)	649.95	**1.52**
AS4/APC2 [5]	$[-45/0/45/90]_{2s}$	38.1	792 (2.78%)	792.45	**0.06**
IM7/8552 [7]	$[90/0/\pm 45]_{3s}$	12	845.1 (1.29%)	854.35	**1.09**
HTA/6376-C [9]	$[45/0/-45/90]_{3s}$	36	710 (2.4%)	708.49	**0.21**
	$[90/0]_{4s}$	36	1110 (1.5%)	1118.1	**0.73**
	$[90/0]_{2s}$	36	1060 (5.2%)	1107.6	**4.49**

In some cases, the literature provides experimental stress-strain curves [8, 16], which can be compared with the evolution of the overall stiffness of the laminate with the DDM model. The comparison between numerical and experimental results of four different materials is shown in Fig. 7. The differences between numerical and experimental stiffness are less than 3.13% (Fig. 7). These curves are linear until failure, typical of laminates with brittle fibre dominated failure, with little or non delamination or fibre splitting.

Therefore, the DDM model can be a useful tool to estimate the failure strength and stiffness in laminates with and without stress concentrations subjected to in-plane loads. The model is applicable to composites with different properties and stacking sequences, when the failure is not controlled by delamination or ply splitting.

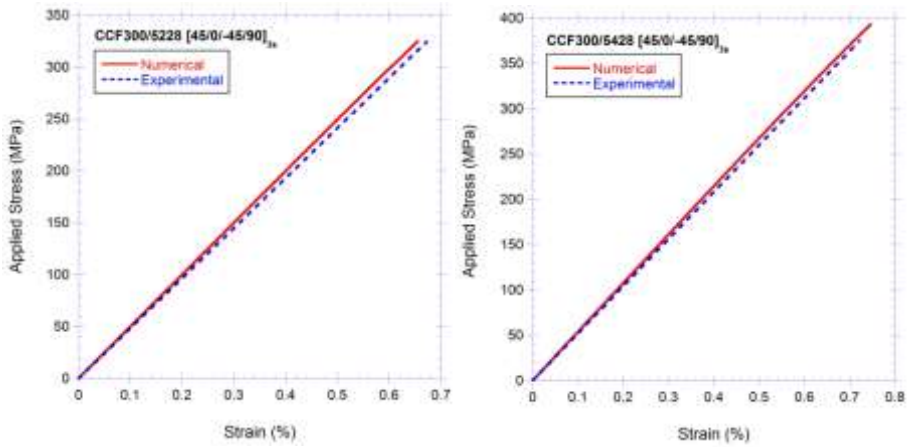

a) b)

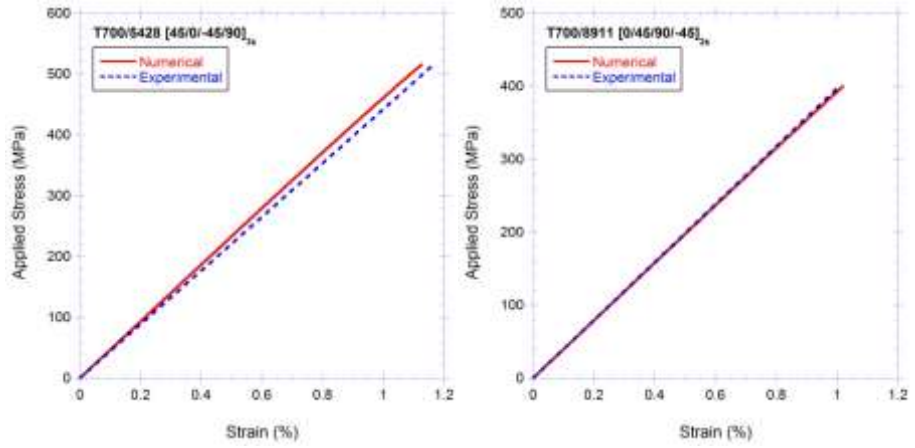

c) d)

Fig. 7. Comparison between numerical and experimental applied stress–strain curve for: a) CCF300/5228 [30], b) CCF300/5428 [30], c) T700/5428 [30] and d) T700/8911 [32].

4. Influence of Weibull modulus on laminate failure

The fibre failure of the laminate is associated to the damage parameter D_1 (Eq. (1)), defined with a Weibull distribution of two parameters [12, Eq. 8.8]. The width of this distribution is controlled by the Weibull modulus (***m***). For un-notched specimens, ***m*** is used as the true Weibull modulus of the fibre tow, whereas for notched specimens ***m*** is used also as a regularization parameter to obtain a smooth distribution of damage across the specimen.

In this work, the influence of the Weibull modulus on matrix and fibre damage evolution and on failure strength of notched and un-notched laminates is analysed. The values of ***m*** studied are between 3 and 9, being this the most common range of variation according to the literature [12, Table 2.3].

To study the influence of ***m***, notched and un-notched laminates with $[90/0/\pm45]_{3s}$ stacking sequence of IM7/8552 are selected. Fig. 8 shows the influence of ***m*** on the applied stress-strain curve, the longitudinal stress on 0º plies (measured in the most loaded Gauss point of the element just above the hole) and the failure strength of the laminate. The width of the laminates is 60 mm and the radius of the hole in the notched laminate is 5 mm.

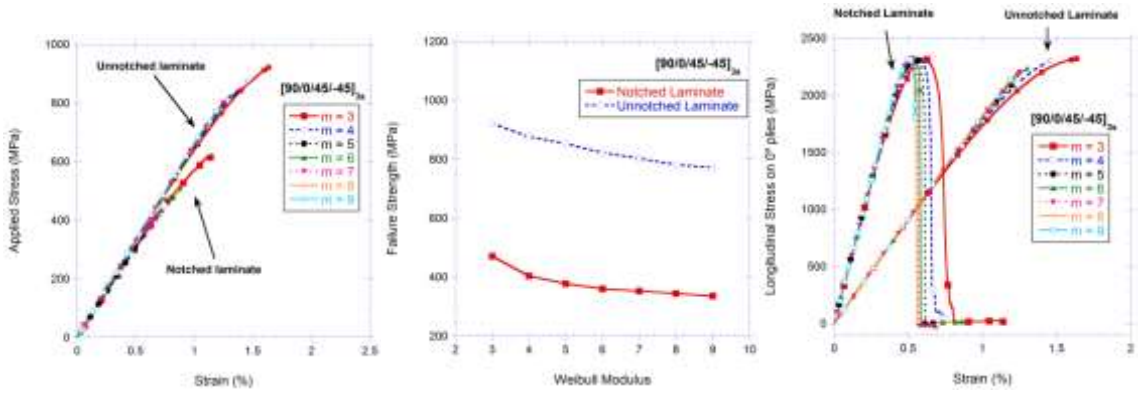

a) b) c)

Fig. 8. Influence of Weibull modulus for notched and un-notched $[0/90/45/-45]_s$ laminate: a) Applied stress over the laminate, b) Failure strength vs Weibull moduls and c) longitudinal stress on 0º plies.

For both notched and unnotched laminates, there is no significant influence of Weibull modulus on the overall stiffness of the laminate, Fig.8a. Increasing the value of ***m,*** the maximum applied stress and strain that can be applied in notched and un-notched laminates decrease. In Fig. 8.b, a reduction of 28.59% in failure strength is observed when the modulus increases from 3 to 9 for the notched laminate while a reduction of 16.17% is observed for the un-notched laminate. Therefore, the effect of ***m*** is more significant in laminates with stress concentrations.

When the Weibull modulus decreases, the Weibull distribution of fibre strength is wider. That means there are more fibres that have a high strength, and more that are very weak. On the analysis, this produces a wider damage area. That reduces the damaged modulus of the 0º laminas over a wider area. Then, it takes more applied strain to get the most solicited Gauss point to reach the tensile strength of the ply in fibre direction (Fig. 8.c). In the meantime, more strain means the rest of the specimen is loaded to a higher strain, and that means it takes more load. The macroscopic effects are lower notch sensitivity and higher failure load, Fig.8b.
Fig. 8.c shows that for low applied strains, below 0.4%, there is no significant influence of the Weibull modulus. Above this strain value, for higher values of ***m*** the slope of the curve increases. In addition, more stress concentration around the edge of the hole appears when the value of ***m*** increase.

Longitudinal damage on 0º plies near the edge of the hole, corresponding to fibre failure are shown in Fig. 9. As the Weibull modulus increase, the extension of the damage area around the edge of the hole decrease, while the stress concentration increase. This behaviour is also observed on 90º and ±45º plies, with the value of damage reached five orders and one order of magnitude lower than the one reached on 0º plies. This behaviour is consistent with the narrower variation in the strength of the fibres afforded by the higher value of ***m***.

For notched laminates, no influence of ***m*** is observed on the initiation of matrix damage in the 90º plies. The onset of matrix damage is insensitive to the value of ***m***. During evolution, an increase in the Weibull modulus produces a decrease of crack density on the element analysed and therefore the damaged area round the hole is smaller. Additionally, no matrix cracking is observed in the 0º and ±45º plies. For unnotched laminates, crack density is uniform over the entire specimen, so ***m*** has no influence.

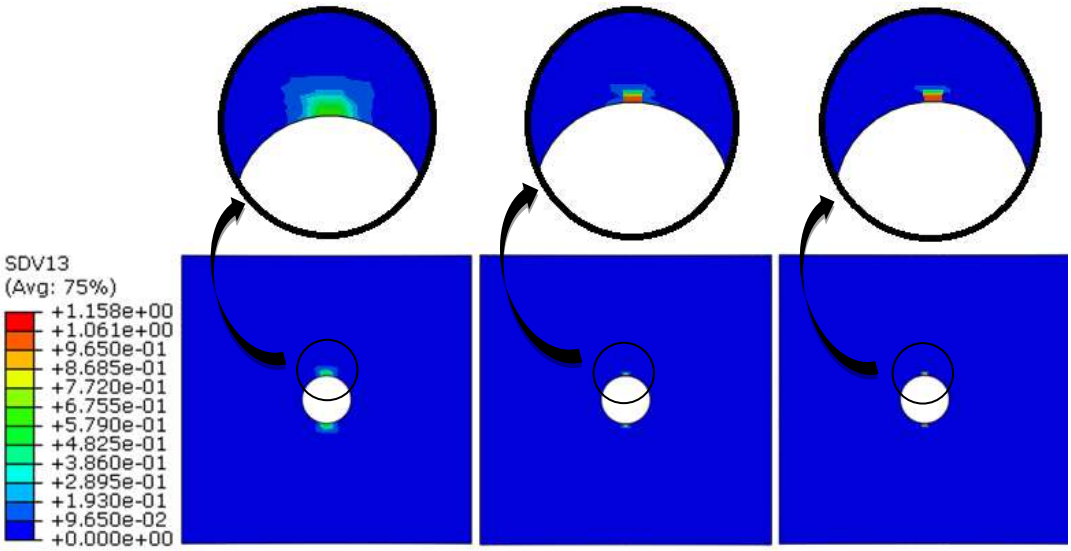

Fig. 9. Longitudinal damage on 0º plies for different values of m (3, 5 and 7 from left to right).

5. Conclusions.

A new algorithm to calculate matrix cracking evolution in the context of the DDM models presented. To improve the numerical convergence, a Regula Falsi method is proposed.

The new implementation of DDM is validated for notched and unnotched laminates. Several materials with different types of carbon fibres and matrices, both thermoset (epoxy) and thermoplastic (PEEK) are analysed. Experimental failure strengths and applied stress-strain curves from the literature are compared with the results obtained with the DDM model. Good approximation is obtained in all the cases studied.

Three criteria to estimate the failure strength are compared: design criterion, local criterion and macro criterion. The Local criterion provides better results in general than the other two criteria when compared with experimental results. Differences in failure strength less than 6.6% are observed between the predictions of the local criterion and experimental data over a wide variety of laminates, materials, and notch geometries.

Weibull modulus (***m***) of the Weibull distribution defined to predict the fibre failure of the laminate is used as a regularization parameter in notched laminates. Its influence over failure strength, applied stress-strain curve, and longitudinal stress is analysed. From the applied stress-strain curve it is observed that the stiffness of the laminate is independent of ***m***. An increase in ***m*** results in a reduction of the failure strength of the laminate, being the influence of ***m*** more significant for macro criterion. For larger values of ***m***, more stress concentration and less failure strength are observed. An increase in ***m*** results in a decrease of the damage extension area for 0º plies around the hole.

Acknowledgement

The authors are indebted for the financial support of this work to the Ministry of Economy and Competitiveness of Spain (project DPI2013-42240-R).

REFERENCES

1. Su ZC, Tay TE, Ridha M, Chen BY. Progressive damage modeling of open-hole composite laminates under compression. Composite Structures 2015; 122:507–517.
2. Erçin GH, Camanho PP, Xavier J, Catalanotti G, Mahdi S, Linde P. Size effects on the tensile and compressive failure of notched composite laminates. Composite Structures 2013;96:736-744.
3. Chen BY, Tay TE, Baiz PM, Pinho ST. Numerical analysis of size effects on open-hole tensile composite laminates. Composites: Part A 2013;47:52-62.
4. Caminero MA, Lopez-Pedrosa M, Pinna C, Soutis C. Damage monitoring and analysis of composite laminates with an open hole and adhesively bonded repairs using digital image correlation. Composites: Part B 2013; 53:76-91.
5. Hallett SR, Green BG, Jiang WG, Wisnom MR. An experimental and numerical investigation into the damage mechanisms in notched composites. Composites: Part A 2009;40:613-624.
6. Camanho PP, Erçin GH, Catalanotti G, Mahdi S, Linde P. A finite fracture mechanics model for the prediction of the open-hole strength of composite laminates. Composites Part A: Applied Science and Manufacturing 2012; 43(8): 1219-1225.
7. Swolfs Y, McMeeking RM, Verpoest I, Gorbatikh L. Matrix cracks around fibre breaks and their effect on stress redistribution and failure development in unidirectional composites. Composites Science and Technology 2015;108:16-22.
8. Swolfs Y, Verpoest I, Gorbatikh L. Issues in strength models for unidirectional fibre-reinforced composites. related to Weibull distributions, fibre packings and boundary effects. Composites Science and Technology 2015;114:42-49.
9. Iarve EV, Mollenhauer D, Kim R. Theoretical and experimental investigation of stress redistribution in open hole composite laminates due to damage accumulation. Composites: Part A 2005;36:163-171.

10. Ogi K, Yashiro S, Takahashi M, Ogihara S. A probabilistic static fatigue model for transverse cracking in CFRP cross-ply laminates. Composites Science and Technology 2009;69:469-476.
11. Nemeth NN. Probability density distribution of the orientation of strength-controlling flaws from multiaxial loading using the unit-sphere stochastic strength model for anisotropy. Int J Fract 2014; 185:97–114.
12. Barbero EJ. Introduction to composite materials design. 2nd ed. Boca Raton, FL: CRC Press, 2011.
13. Camanho PP, Maimí P, Dávila CG. Prediction of size effects in notched laminates using continuum damage mechanics. Composite Science and Technology 2007;67:2715-2727.
14. Orifici AC, Herszberg I, Thomson RS. Review of methodologies for composite material modelling incorporating failure. Composite Structures 2008;86:194-210.
15. Sadeghi G, Hosseini-Toudeshky H, Mohammadi B. An investigation of matrix cracking damage evolution in composite laminates – Development of an advanced numerical tool. Composite Structures 2014;108:937-950.
16. Liu PF, Zheng JY. Recent developments on damage modeling and finite element analysis for composite laminates: A review. Materials and Design 2010;31:3825-3834.
17. Whitney JM, Nuismer RJ. Stress fracture criteria for laminated composites containing stress concentrations. J Compos Mater 1974;8:253-265.
18. Balacó de Morais A. Open Tensile strength of quasi-isotropic laminates. Composite Science and Technology 2000; 60:1997-2004.
19. Barbero EJ, Lonetti P. Damage Model for Composites Defined in Terms of Available Data. Mechanics of composite materials and structures 2001;8(4):299-315.
20. Barbero EJ, Cortes DH. A mechanistic model for transverse damage initiation, evolution, and stiffness reduction in laminated composites. Composites Part B 2010; 41:124-32.
21. Hinton MJ, Soden PD. Predicting failure in composite laminates: the background to the exercise. Composite science and thecnlogy 1998; 58: 1001-1010.
22. Moure MM, Sanchez-Saez S, Barbero E, Barbero EJ. Analysis of damage localization in composite laminates using a discrete damage model. Composites Part B 2014; 66: 224-232.
23. Abaqus Simulia manual.
24. Seng C. Tan. A progressive Failure Model for Composite Laminates Containing Openings. Journal of Composite Materials 1991;25(5):556-577.
25. Pinnell MF. An examination of the effect of composite constituent properties on the notched-strength performance of composite materials. Composite Science and Technology 1996;56:1405-1413.
26. Green BG, Wisnom MR, Hallett SR. An experimental investigation into the tensile strength scaling of notched composites. Composites: Part A 2007;38:867-878.

27. Maimí P, Camanho PP, Mayugo JA, Dávila CG. A continuum damage model for composite laminates: Part II-Computational implementation and validation. Mechanics of Materials 2007; 39: 909-919.
28. Material data sheet provided by. www.ides.com
29. Lagace PA, Bhat NV, Gundogdu A. Response of notched graphite/epoxy and graphite/peek systems. Composite Materials: Fatigue and Fracture, Fourth Volume, ASTM STP 1156, 1993. p. 55-71.
30. Xing L, Zhidong F, Zengshan L, Lu L. A new stress-based multi-scale failure criterion of composites and its validation in open hole tension tests. Chinese Journal of Aeronautics 2014;27:1430–1441.
31. O'Higgins RM, McCarthy MA, McCarthy CT. Comparison of open hole tension characteristics of high strength glass and carbon fibre-reinforced composite materials. Composites Science and Technology 2008;68: 2770-2778.
32. Liu PF, Chu JK, Liu YL, Zheng JY. A study on the failure mechanisms of carbon fibre/epoxy composite laminates using acoustic emission. Materials and Design 2012;37:228-235.

FIGURE CAPTION

Fig.1. Fibre Failure algorithm scheme
Fig.2. Matrix cracking implementation
Fig.3. Regula Falsi algorithm implemented.
Fig. 4. Laminate implementation scheme of the combined formulation.
Fig. 5. Discretization of notched and un-notched laminates.
Fig. 6. Definition of the three criteria used to estimate the failure strength of the notched laminates.
Fig. 7. Comparison between numerical and experimental applied stress–strain curve for: a) CCF300/5228 [8], b) CCF300/5428 [8], c) T700/5428 [8] and d) T700/8911 [16].
Fig. 8. Influence of Weibull modulus for notched and un-notched $[0/90/45/-45]_s$ laminate: a) Applied stress over the laminate, b) Failure strength vs Weibull moduls and c) Longitudinal stress on 0º plies.
Fig. 9. Longitudinal damage on 0º plies for different values of m (3, 5 and 7 from left to right).

TABLE CAPTION

Table 1. Material properties of the composite materials analysed I
Table 2. Material properties of the composite materials analysed II
Table 3. Failure strength for notched laminates.
Table 4. Failure strength for un-notched laminates.